EPJ Web of Conferences **60**, 14009 (2013)
DOI: 10.1051/epjconf/20136014009

Studies of Soft QCD at LHCb

Alexandru T. Grecu (on behalf of the LHCb Collaboration)[1,a]

[1] *"Horia Hulubei" National Institute for Physics and Nuclear Engineering, Reactorului 30, P.O.B. MG-6, RO-077125, Bucharest-Măgurele, Romania, EU*

Abstract. Due to its unique pseudorapidity coverage and the possibility of extending measurements to low transverse momenta, LHCb provides important input to the understanding of particle production in a kinematic range where QCD models have large uncertainties. Measurements of charged, strange and charmed particle production and energy flow are performed in the approximate pseudorapidity range $2 < \eta < 5$, which corresponds to the acceptance of the LHCb spectrometer. The results are compared to predictions given by several Monte Carlo event generators.

1 Introduction

The LHCb detector[1], one of the four major experiments at the Large Hadron Collider (LHC), was designed to perform precise measurements of CP-violating and rare decay processes involving hadrons that contain the beauty (b) and charm (c) quarks. To take advantage of the topology of the $b\bar{b}$ pair production, the detector is a single-arm forward spectrometer with a unique pseudorapidity coverage ($2.0 < \eta < 5.0$) which partially overlaps the central pseudorapidity domains accessible to the general purpose detectors of ATLAS and CMS. It runs at a low and constant number of visible proton-proton (pp) interactions. Its high precision tracking system consists of a silicon-strip vertex detector (VELO) enclosing the primary pp interaction region and a large area silicon tracker located upstream of a magnetic dipole with a bending power of approximately 4 Tm, and three stations of silicon-strip detectors and straw drift tubes situated downstream. The larger angular acceptance of the VELO allows reconstruction of backward tracks in the pseudorapidity range $-4 < \eta < -1.5$ which have no momentum information and are not influenced by the LHCb magnet. Charged hadrons are identified by two ring-imaging Cherenkov detectors, one placed before the magnet to cover the low and intermediate momentum (p) range and the second downstream of the magnet to measure particles of high momentum propagating at low polar angles. A calorimetry system consisting of scintillating-pad and preshower detectors followed by an electromagnetic (ECAL) and a hadronic calorimeter (HCAL) is used to characterize the photon, electron and hadron candidates. The muons are detected by a specialized system composed of alternating layers of iron and multi-wire proportional chambers. The trigger includes a hardware stage based on information from the calorimeter and muon systems and a software stage in which a full event reconstruction is performed. The results presented in these proceedings were obtained from analyses performed on events that passed the trigger with a minimal requirement of having at least one track reconstructed in the LHCb detector acceptance. Simulated data were used to calculate efficiencies, estimate systematic uncertainties and to provide predictions to compare against measurements. These samples were produced using PYTHIA [2, 3] Monte Carlo (MC) generators set up according to established [3, 4] or specific LHCb [5] MC configurations in order to generate pp collisions. Specific hadron decays are handled by EVTGEN [6] with final state radiation simulated by PHOTOS [7]. The generated particles were transported through the detector using the GEANT4 [8, 9] tool-kit which performs the interaction with the material and yields the response of the detector as described in [10]. Widely used generators in the cosmic ray experimental community [11–13] as well as various theoretical estimation schemes [14, 15] were also employed to produce samples for further comparisons with experimental data.

The high precision tracking and vertexing, very good momentum resolution and excellent performance of the ring imaging Cherenkov system [16] enable the LHCb collaboration to extend the range of measurements done by other experiments toward low longitudinal momentum fraction x [17] and momentum transfer (Q^2) where unique nonperturbative quantum chromodynamics (QCD) studies are possible. These proceedings present the latest results of soft QCD analyses performed on minimum-bias data collected in low luminosity runs in 2010 at energies of 0.9 and 7 TeV. These analyses follow previous LHCb studies on similar topics [18–21].

2 Forward Energy Flow

The energy flow (EF) is a valuable observable in probing the multi parton interactions (MPI) and determining the

[a] e-mail: alexandru.grecu@nipne.ro

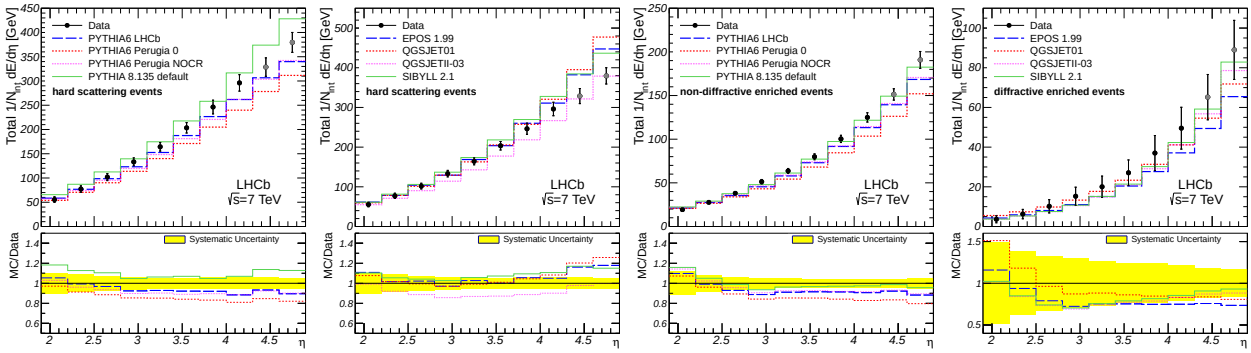

Figure 1. Total energy flow as function of η for the indicated event classes. The corrected measurements are represented by points with error bars (only systematic uncertainties as statistical errors are negligible) while the generator predictions are shown as histograms. The MC to data ratios are also given. Data points estimated with MC constraints are shown in grey (see [22] for further details).

amount of final state radiation which contributes to the underlying event in hadron-hadron collisions. The EF is defined as

$$\frac{1}{N_{\rm int}}\frac{{\rm d}E_{\rm tot}}{{\rm d}\eta},$$

where $N_{\rm int}$ is the number of inelastic pp interactions and ${\rm d}E_{\rm tot}$ is the (charged or total) energy of stable particles in each ${\rm d}\eta$ range. It may be used in tuning generators both for collider and cosmic ray physics. Experimentally it is determined as the average energy of the stable particles in each η bin normalised by the bin size. Events with multiple primary vertices, high pile-up events, are estimated to account for approximately 5% of the statistics corresponding to the 0.1 nb^{-1} integrated luminosity analysed. Four categories of events are considered. All selections start from a global (1) inclusive minimum bias class of events with at least one reconstructed track with $p > 2$ GeV/c. These events are further classified as (2) hard scattering, imposing the existence of at least one well reconstructed track with transversal momentum (p_T) higher than 3 GeV/c, (3) diffractive enriched, searching for events with no backward tracks as the experimental signature of the characteristic rapidity gap and (4) non-diffractive enriched, when the presence of at least one backward track is required. The charged particle EF is measured using only the momentum information from the tracking system. The total EF is obtained by adding to the charged EF the contribution of the neutral component in data which is estimated by applying constraints from simulation and using information from the ECAL. The uncertainties come mainly from differences in tracking efficiencies between data and simulation, the presence of pile-up events and the models considered in simulation to correct the raw data for detector effects. Some results of the analysis are shown in Fig. 1 for the total EF. The following conclusions apply also to the charged EF as detailed in [22]. The PYTHIA 6 tunes underestimate the EF for all event classes, especially at high η, while the PYTHIA 8.135 default tune is in better agreement with the experimental points except for the hard scattering event class. The high energy cosmic ray generators have the tendency to overestimate the data except for the class of diffractive enriched events where simulated points are below the experimental ones and similar to the PYTHIA predictions. Among them SIBYLL [13] and EPOS [11] give a better estimate of the total EF, with SIBYLL closely following the PYTHIA 8 behaviour. In the class of hard scattering events QGSJETII-03 [12] offers the closest description of the total EF.

3 Prompt Light Hadron Production Ratios

The charged light hadron production ratios, recently measured by the LHCb collaboration [23], are important observables to test MC generator tuning besides particle multiplicities and kinematic distributions of inclusive particles or individual particle species in each event. The same-particle ratios are also of particular interest to probe the baryon-number transport process, modelled by mechanisms in which Pomeron exchange plays a significant role, but where the influence of other sources such as the odderon is not yet fully determined (see references within [23]). At the same time, the different-particle ratios provide direct information for optimizing generator parameters related to baryon-to-meson suppression and flavour production. The study was performed on data collected in low pile-up LHC runs at 0.9 TeV and 7 TeV corresponding to an integrated luminosity of 0.3 nb^{-1} and 1.8 nb^{-1}, respectively, and considering the following particle ratios

$$\frac{\bar{p}}{p}, \frac{K^-}{K^+}, \frac{\pi^-}{\pi^+}, \frac{p+\bar{p}}{\pi^+ + \pi^-}, \frac{K^+ + K^-}{\pi^+ + \pi^-}, \frac{p+\bar{p}}{K^+ + K^-}.$$

Only particles originating directly from the primary interaction or from subsequent decays of resonances (*prompt* particles) are considered. A sample of data collected at 7 TeV, consisting of decays $K^0_S \to \pi^+\pi^-$, $\Lambda \to p\pi^-$ (c.c.) and $\Phi \to K^+K^-$ was used for the calibration of the particle identification (PID). Simulated events, produced with the LHCb MC configuration and reconstructed as detailed in section 1, were used to apply corrections accounting for non-prompt contamination, geometrical acceptance losses and track finding inefficiency. The last is the most important effect. They were also used to validate the analy-

sis procedure and estimate most of the systematic uncertainties. The latter are mainly due to the PID efficiency being proportional to the size of the calibration sample. Other sizeable uncertainties are related to the different interaction cross-sections, the amount of detector material traversed by the candidates, tracking efficiency and non-prompt contamination estimations. It is found that none of the PYTHIA 6 "Perugia tunes" [4] describe the data satisfactorily, the largest discrepancies appearing in the different-particle ratios involving prompt pions especially at high p_T (see Fig. 3). The "Perugia tunes" behaviour is however in good agreement with previously published comparisons of strangeness production and antiparticle-to-particle ratios [19, 20]. In general, the LHCb MC tune [5] seems to better describe the data.

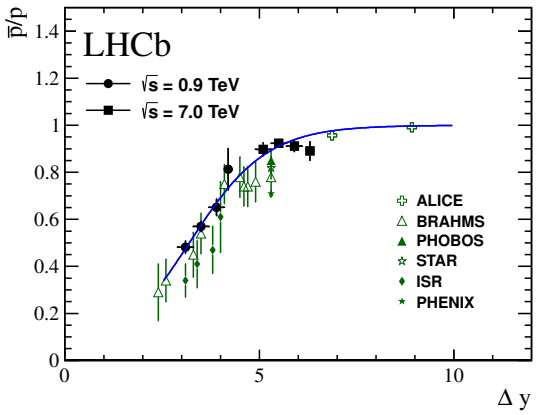

Figure 2. Results for $\bar{p}/p$ ratio as function of Δy from LHCb and other experiments [24–28]. A fit to the LHCb and ALICE measurements [24] is superimposed (from [23]).

The $\bar{p}/p$ ratio was also studied as a function of rapidity loss (Δy), the difference between the particle rapidity y and the rapidity of the beam y_{beam}, in the interval 3.1 to 6.3. Precise measurements are obtained in agreement with other experiments as shown in Fig. 2. Combining the LHCb and ALICE measurements, a fit on a simple model based on Regge theory is performed, the result excluding the association between string junction and the odderon in baryon number transport at high energies in the forward region.

4 Prompt Charm Production at LHCb

Measurements of charmed hadron production cross-sections provide valuable input in testing the QCD fragmentation and hadronisation models, in particular next-to-leading order calculation methods such as the Generalised Mass Variable Flavour Number Scheme (GM-VFNS) [15] or the fixed order next-to-leading-log resummation (FONLL) [14] approach. We summarize below the measurements with the LHCb detector of the D^0, D^+, D^{*+}, D_s^+ and Λ_c^+ production in pp collisions at a centre-of-mass energy of 7 TeV, in the phase-space domain characterized by $2.0 < y < 4.5$ and $p_T < 8$ GeV/c. The analysed data corresponds to an integrated luminosity of 15 nb^{-1} recorded in 2010, having about 1.1 visible pp interactions per triggered bunch crossing. Only primary/prompt charmed hadrons produced either directly at the primary interaction vertex or through decays of excited charm resonances are considered, the secondary charm products from decays of b-hadrons being treated as background. The candidate selection criteria was tuned independently for each decay. A series of fits are performed in order to disentangle the prompt signal from secondary charmed hadrons and combinatorial background, and in the case of D^{*+} from two additional types of backgrounds due to mismatch between the D^0 and slow pion candidates used in reconstruction. The PID efficiency is determined for each charmed hadron decay mode combining information from high purity data samples and simulated decays while the efficiencies for the rest of the selection criteria is obtained from studies with full event simulation. The uncertainties are split in three categories: globally correlated contributions from the uncertainty on measured luminosity and on the tracking efficiency, sources correlated between bins but uncorrelated between decays modes and sources that are uncorrelated between bins and decays modes. The systematic uncertainties on the PID efficiency and branching fractions are considered bin-correlated. Systematic uncertainties of the reconstruction and selection efficiencies and of the yield determination fall into both bin-correlated and uncorrelated classes so separate values are evaluated, where possible for each bin. The uncertainty sources are uncorrelated so they can be summed in quadrature for each bin of each decay mode (see table 1 in [29]). The analysis procedure is validated on alternative decay modes and a selection of D^0 decays that does not use PID information. The differential cross-sections are measured as function of p_T and y discarding the bins with insufficient statistics to produce a reliable measurement.

Two theoretical approaches are used to give charmed hadron production cross-section estimations which were successfully compared to data from Tevatron [30] and ALICE [31–33]. The theoretical uncertainties due to charm quark mass and renormalisation and factorisation scales for FONLL are not shown in Fig. 4. Besides in this approach the values of the transition probabilities for charm quark to exclusive hadron state are taken from measurements performed in e^+e^- experiments assuming they apply to hadron collisions as well. A similar assumption is done in GM-VFNS when performing the convolution with fragmentation function describing the $c \to H_c$ transition resulted from a fit to data measured at e^+e^- colliders in order to obtain the total transition probabilities. Uncertainties due to scale variations were computed only for the D^0 production and assumed the same in relative size for the other hadron species. Results were provided only for $p_T > 3$ GeV/c. The theoretical curves in Fig. 4 are smooth and the value at the bin centre corresponds to the differential cross-section calculated in that bin so that the comparison to data is straightforward. A good agreement is observed the measured points being enveloped between the values estimated by FONLL and GM-VFNS. In calcu-

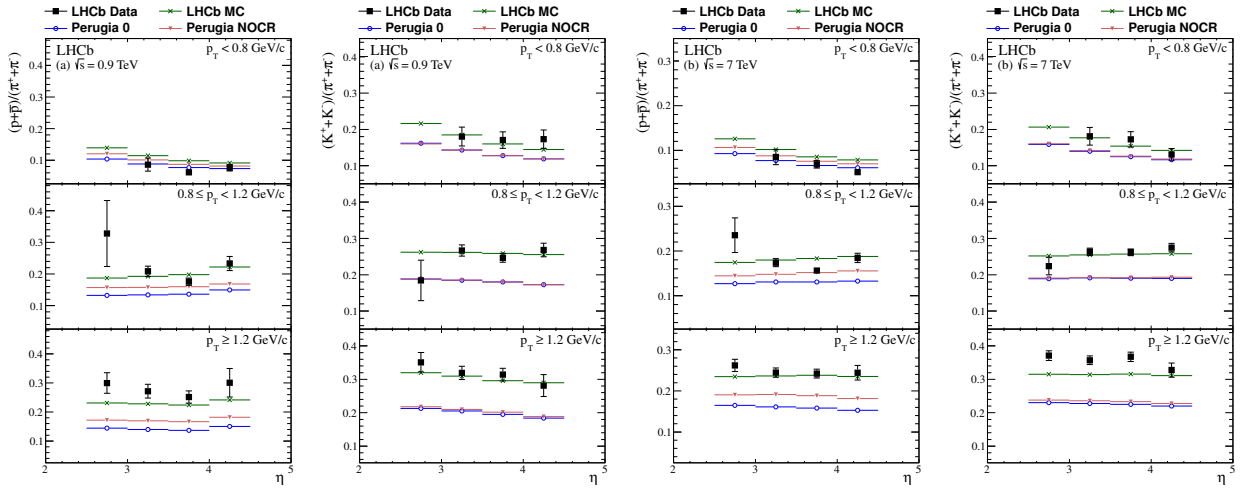

Figure 3. From left to right, the results for the $(p + \bar{p})/(\pi^+ + \pi^-)$ and $(K^+ + K^-)/(\pi^+ + \pi^-)$ at 0.9 TeV and 7 TeV, respectively. Further ratios are given in [23].

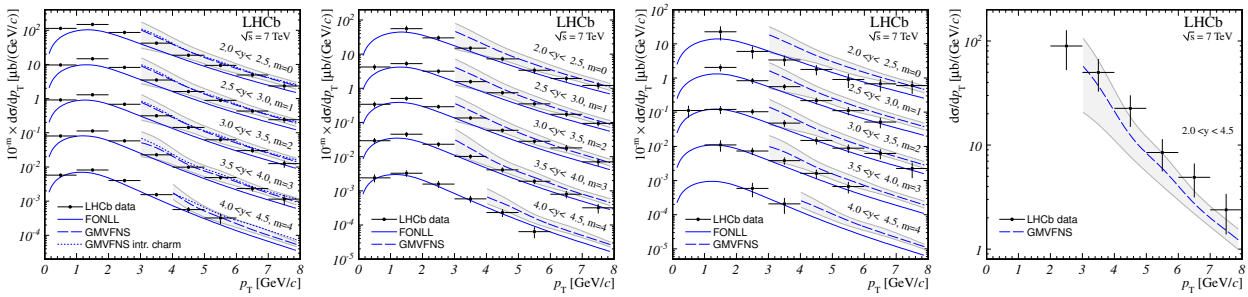

Figure 4. From left to right, differential cross-sections for D^0, D^+, D_s^+ and Λ_c^+ charmed hadrons compared to theoretical predictions as functions of p_T in different y domains. Each curve and associated data points correspond to a particular y range and are scaled by a factor 10^{-m} with the exponent and range indicated. The experimental point error bars contain the sum of statistical ans systematic errors, while the shaded regions determine the extent of theoretical uncertainties for the GM-VFNS prediction (see [29] for details).

lating the integral cross-sections and their ratios, the low statistics bins with relative uncertainty on the yield exceeding 50% are eliminated and the cross-sections are extrapolated with predictions given by simulation. These results are tabulated in [29]. When combining the five individual cross-sections taking into account the correlation factors to determine the total charm cross-section, a correction factor of $1/2$ must be applied to eliminate the effect of ignoring the charge conjugation. The value for the prompt charm production cross-section inside the acceptance of this study ($p_T < 8$ GeV/c, $2.0 < y < 4.5$) is

$$\sigma(c\bar{c}) = 1419 \pm 12(\text{stat}) \pm 116(\text{syst}) \pm 65(\text{frag})\ \mu\text{b},$$

where the final error is due to the fragmentation functions.

5 Conclusions

Although it was designed to probe specific physics phenomena in the b and c quark sector, the LHCb detector proves to be a very flexible instrument that has also allowed studies of non-perturbative QCD to be made in the forward region. The results above give new insights on the processes contributing to the underlying event and on the limits of the fragmentation and hadronisation models. Thus, the comparison of the energy flow measurements to the MC models proves that the diffractive processes play a vital role in the description of multi-parton interactions especially at the LHC energies where inelastic processes between soft partons become sufficiently energetic to influence the final state particle production. Measurements of antibaryon-to-baryon ratios give substantial information in understanding the baryon production and transport phenomena by testing consacrated theoretical models. At the same time these results provide important reference for future MC generator tuning in elementary particle as well as high energy cosmic ray physics. The studies of the charmed hadron production cross-sections brought a solid confirmation of a couple of perturbative calculation approaches for these observables, giving hints for future improvements of the QCD fragmentation and hadronisation models these schemes are based on.

References

[1] A.A. Alves Jr., et. al (LHCb Collab.), J. Instrum. **3**, S08005 (2008)

[2] T. Sjöstrand, S. Mrenna, P. Skands, J. High Energy Phys. **05**, 026 (2006)

[3] T. Sjöstrand, S. Mrenna, P. Skands, Comput. Phys. Commun. **178**, 852 (2008)

[4] P.Z. Skands, Phys. Rev. D **82**, 074018 (2010)

[5] I. Belyaev, T. Brambach, N.H. Brook, N. Gauvin, G. Corti, K. Harrison, P.F. Harrison, J. He, P.H. Ilten, C.R. Jones et al., *Handling of the generation of primary events in GAUSS, the LHCb simulation framework*, in *Nuclear Science Symposium Conference Record (NSS/MIC)* (IEEE, New York, 2010), p. 1155

[6] D.J. Lange, Nucl. Instrum. Meth. A **462**, 152 (2001)

[7] P. Golonka, Z. Was, Eur. Phys. J. C **45**, 97 (2006)

[8] S. Agostinelli, et. al (GEANT4 Collab.), Nucl. Instrum. Meth. A **506**, 250 (2003)

[9] J. Allison, et. al (GEANT4 Collab.), IEEE Trans. Nucl. Sci. **53**, 270 (2006)

[10] M. Clemencic, G. Corti, S. Easo, C.R. Jones, S. Miglioranzi, M. Pappagallo, P. Robbe, J. Phys.: Conf. Ser. **331**, 032023 (2011)

[11] T. Pierog, K. Werner, Nucl. Phys. Proc. Suppl. **196**, 102 (2009)

[12] S. Ostapchenko, AIP Conf. Proc. **928**, 118 (2007)

[13] E.J. Ahn, R. Engel, K.G. Thomas, P. Lipari, T. Stanev, Phys. Rev. D **80**, 094003 (2009)

[14] M. Cacciari, S. Frixione, N. Houdeau, M.L. Mangano, P. Nason, G. Ridolfi, J. High Energy Phys. **1210**, 137 (2012)

[15] B. Kniehl, G. Kramer, I. Schiebein, H. Spiesberger, Eur. Phys. J. C **72**, 2082 (2012)

[16] M. Adinolfi, et al. (LHCb RICH group), Eur. Phys. J. C **73**, 2431 (2013)

[17] J.D. Björken, E.A. Paschos, Phys. Rev. **185**, 1975 (1969)

[18] R. Aaij, et al. (LHCb Collab.), Phys. Lett. B **693**, 69 (2010)

[19] R. Aaij, et al. (LHCb Collab.), J. High Energy Phys. **08**, 034 (2011)

[20] R. Aaij, et al. (LHCb Collab.), Phys. Lett. B **703**, 267 (2011)

[21] R. Aaij, et al. (LHCb Collab.), Eur. Phys. J. C **72**, 1947 (2012)

[22] R. Aaij, et al. (LHCb Collab.), Eur. Phys. J. C **73**, 2421 (2013)

[23] R. Aaij, et al. (LHCb Collab.), Eur. Phys. J. C **72**, 2168 (2012)

[24] K. Aamodt, et al. (ALICE Collab.), Phys. Rev. Lett. **105**, 072002 (2010)

[25] I.G. Bearden, et al. (BRAHMS Collab.), Phys. Lett. B **607**, 42 (2005)

[26] B.B. Back, et al. (PHOBOS Collab.), Phys. Rev. C **71**, 021901 (2005)

[27] B.I. Abelev, et al. (STAR Collab.), Phys. Rev. C **79**, 034909 (2009)

[28] S.S. Adler, et al. (PHENIX Collab.), Phys. Rev. C **74**, 024904 (2006)

[29] R. Aaij, et al. (LHCb Collab.), Nucl. Phys. B **871**, 1 (2013)

[30] D. Acosta, et al. (CDF Collab.), Phys. Rev. Lett. **91**, 241804 (2003)

[31] B. Abelev, et al. (ALICE Collab.), J. High Energy Phys. **1207**, 191 (2012)

[32] B. Abelev, et al. (ALICE Collab.), Phys. Lett. B **718**, 279 (2012)

[33] B. Abelev, et al. (ALICE Collab.), J. High Energy Phys. **1201**, 128 (2012)